

Integrated surface geophysical approach to locate a karst conduit: a case study from Royal Spring Basin, Kentucky, USA

***G. N. Tripathi¹ and A. E. Fryar²**

¹*Department of Mines and Geology, Ministry of Industry, Government of Nepal*

²*Department of Earth and Environmental Sciences, University of Kentucky, Lexington, KY 40506-0053 USA*

(*Email: ganeshtri@gmail.com)

ABSTRACT

Groundwater flow in karst terrains is difficult to map because it can be concentrated through conduits that do not necessarily coincide with the surface features. We applied electrical resistivity (ER) and self-potential (SP) techniques at three sites to locate an inferred trunk conduit feeding a major spring in the Inner Bluegrass region of Kentucky (USA). Royal Spring is the primary water supply for the city of Georgetown; the upper part of its basin coincides with the Cane Run watershed. ER profiles (972 m total length) were measured using a dipole–dipole electrode configuration with 2- to 3-m spacing. SP measurements were taken along those ER lines and an additional test profile (230 m) using one stationary reference electrode and another roving electrode at a fixed interval. The SP technique has been used by many researchers to detect the electrokinetic potential generated by groundwater flow. The low resistivity of water in the conduit, as compared to the high background resistivity of limestone bedrock, was the ER exploration target. A negative SP anomaly corresponded to a low ER anomaly for most of the profiles, but a few are not comparable. Although SP data collected over multiple days along the test profile differed significantly, they showed similar trends. Field drift in SP data was found to be highly sensitive to temperature changes during the time of measurement. Although the overall trends of the final SP profiles for different dates were similar, the SP magnitudes varied with the amount of precipitation and the average soil temperature. The low-resistivity anomalies in the 2D inverted sections and corresponding negative SP anomalies at two sites (Berea Road and Kentucky Horse Park) encountered water-filled conduits, although mud-filled voids encountered during drilling at University of Kentucky Agricultural Research Farm sites suggest that these may be tributary conduits rather than the trunk conduit.

Keywords: Electrical resistivity, self-potential, karst, Kentucky, USA

Received: 15 August 2015

Revision accepted: 1 May 2016

INTRODUCTION

Groundwater in karst

Karst is a term commonly associated with carbonate rocks, but other soluble rocks, such as evaporites, gypsum and anhydrite, are also susceptible to development of karst features (Bakalowicz 2005). Karst is developed on carbonate rocks when mildly acidic water (containing dissolved CO₂) dissolves the rock mass along preferential flowpaths. Groundwater transports the dissolution products and simultaneously enlarges the flowpaths (joint, fractures, bedding surfaces, grain boundaries, etc.), thus creating voids and conduits (Bakalowicz 2005). The voids formed may be occluded with sediments deposited following storm events. Like water-filled voids, sediments filled voids generally exhibit a low-resistivity anomaly.

In granular aquifers, groundwater flow paths are commonly delineated by mapping distribution of hydraulic heads from observation wells or piezometers. However, in karst aquifers flow paths are difficult to map because of the extreme heterogeneity of karstified rocks (Bakalowicz 2005). Multiple researchers have sought to define and characterize karst aquifers using different techniques (Romanov et al. 2002; White 2002; Motyka 1998; John et al. 2006; Kiraly 2003; White and White 2005).

Integrated geophysical techniques in karst

Geophysical methods such as electrical resistivity (ER), self-potential (SP), ground penetrating radar (GPR), electromagnetic induction (EM), microgravity and seismic refraction/reflection can aid in identifying and delineating subsurface voids in karst terrains. The SP method has been widely used in groundwater flow studies due to its effectiveness in detecting subsurface water movement. The natural electric potential difference produced by streaming, or electrokinetic potential due to the underground movement of water, is more efficiently detected by the SP method than by any other geophysical technique. Laboratory experiments to study the streaming potential generated by water movement through different geologic media have been performed by Ahmad (1964) and Bogoslovsky and Ogilvy (1972). Ahmad (1964) investigated the streaming potential generated due to water movement through unconsolidated rock while the laboratory experiments on fissured media models by Bogoslovsky and Ogilvy (1972) expanded the scope of streaming potential to the study of karst groundwater flow. Unlike other geophysical techniques, relative SP amplitude along the same survey line varies significantly with time while preserving an overall trend, and in most cases the variations can be related to hydrogeological and meteorological parameters (Ernstson and

Scherer 1986). Corwin (1990) has given a more detailed account of the SP field techniques in environmental and engineering applications. Either positive or negative SP expressions can be expected over cave passages. These expressions could be related to the downward filtration effect through the cave walls and ceilings; movement toward the surface by capillary action; streaming potential of flowing water in conduits; and/or the pH of the electrolyte (Lange and Kilty 1991, Ishido and Mizutani 1981). Lange and Kilty (1991) described many case studies of SP response over caverns in different parts of the United States and possible effects from artificial current sources such as cathodic protection devices on pipelines. Wanfang et al. (1999) developed a methodology to remove the topographic effect from SP data and applied it to identify discrete recharge zones for a karst aquifer. Concentrated vertical groundwater movement through sinkholes produces a significant negative anomaly for an uncontaminated karst aquifer. Several attempts have been made to quantify surface SP data to reproduce reliable subsurface information both in the lab and in the field. A method to interpret the surface SP data quantitatively by determining the shape factor of an anomaly has been tested on synthetic data with and without noise component and implemented for a field data set (El-Araby 2004). Fagerlund and Heinson (2003) utilized the SP method in the laboratory and in the field to determine drawdown and other aquifer parameters.

Various studies have documented the application and limitations of ER surveys in karst environments. The effectiveness of different electrode arrays in ER surveys differs with the properties of the geological target, and depth and selection of an appropriate electrode array are of prime importance in getting reliable subsurface information (Zhou et al. 2002). Those authors compared Wenner, Schlumberger and dipole-dipole electrode arrays to study potential karst hazards associated with sinkholes and found the dipole-dipole array to be the most appropriate technique in such studies. Roth and Nyquist (2003) evaluated the applicability of the multi-electrode earth resistivity technique in karst, comparing several resistivity sections obtained from Wenner, dipole-dipole and Schlumberger arrays with the boring results. Roth and Nyquist (2003) found that the likelihood of locating subsurface voids depended on the spacing and orientation of the ER transects. Schwartz and Schreiber (2009) quantified potential recharge through mantled sinkholes using differential electrical tomography using the dipole-dipole technique. Meyerhoff et al. (2012) used time-lapse ER to track the movement of dilute rainwater through a karst conduit.

SP in conjunction with ER was found to be effective for locating sinkholes and crypto-sinkholes in chalk karst in northwestern France (Jardani et al. 2006). Those authors compared the SP results measured during spring and summer and found negative SP anomalies associated with the same sinkholes and crypto-sinkholes, but the number and magnitude of anomalies were reduced in the summer data. In a lab

experiment, the SP technique was more reliable than ER in locating a thick conductor buried at different orientations (Adeyemi et al. 2006). In general, the usefulness of a geophysical technique can vary depending on the depth and geometry of the target feature, the composition and thickness of overlying soils, and whether the feature is water-filled or not.

Site description

The Inner Bluegrass region of central Kentucky is characterized by karstic features developed within limestone bedrock. The Cincinnati Arch, which is a major regional geological structure in the region, controls the overall gentle dip of the bedrock strata. This north-south trending arch forms the Jessamine and Nashville domes along its axis, which are separated by a saddle in Cumberland County, Kentucky (Nosow and McFarlan 1960). The general stratigraphic sequence of this area consists of the Ordovician-era High Bridge Group, Lexington Limestone and Clays Ferry Formation in ascending order. The High Bridge Group is sub-divided into the Camp Nelson Limestone, Oregon Limestone and Tyrone Limestone (Cressman 1965). A disconformity separates the Lexington Limestone from the underlying Tyrone Limestone. The Lexington Limestone is sub-divided mainly on the basis of lithologic characteristics into 11 members (Cressman 1967).

One of the largest groundwater basins in the Inner Bluegrass region, and perhaps the most studied, is the Royal Spring basin. Royal Spring, which is the main water supply for the city of Georgetown, emerges from the Grier Member of the Lexington Limestone. Prior investigations of the Royal Spring basin have been tended to use tracer techniques and wells (Thraikill et al. 1982, 1991, Hamilton 1950, Matson 1909). In particular, Sullivan (1983) studied the relationship between velocity and discharge, conduit geometry and type of flow using fluorescent dyes. Spangler et al. (1982) reported that all of their dye introduction points (mainly swallets) were within the Grier or Tanglewood member and interpreted the conduit or conduits to have developed within a narrow stratigraphic interval. Thraikill and Gouzie (1984) conducted preliminary field studies to determine discharge and travel time in the basin and also tried to estimate the trunk conduit geometry. Paylor and Currens (2004) determined and mapped groundwater travel times to Royal Spring for a range of discharge values.

Several geophysical studies have been conducted to estimate the geometry, depth and orientation of conduits in the Royal Spring basin. Bonita (1993) collected ER data to establish the subsurface lithostratigraphy of the area and correlated it with the standard lithostratigraphic section. The author concluded that the groundwater basin underlies highly fractured areas and the interbasin underlies less fractured areas. Graham (2000) tested the ER survey technique on a known karst feature (Marshall Spring, Scott County) and applied it at the Kentucky Horse Park. A drillhole in the area encountered a water-bearing conduit, which the author interpreted as feeding Royal Spring.

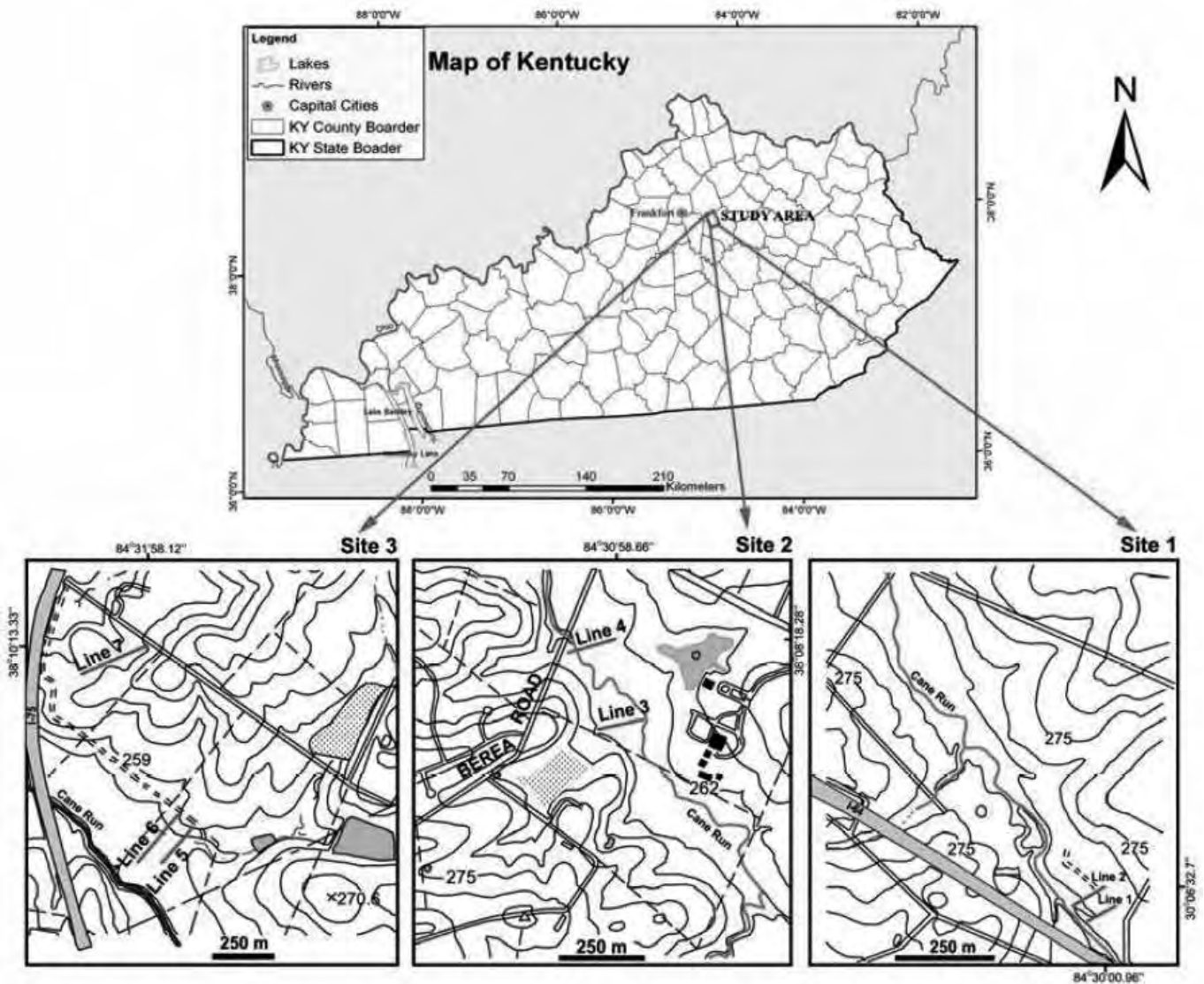


Fig. 1: Map showing geophysical survey lines at study sites (1, UK Agricultural Research Farm; 2, Berea Road; 3 Kentucky Horse Park).

Zhu et al. (2011) built on the work of Graham (2000) by conducting 2-D, quasi 3-D, and time-lapse ER in dipole-dipole mode to locate resistivity anomalies, some of which were targeted for drilling. In particular, a major water-filled conduit was penetrated near an ER anomaly, although similar anomalies were associated with water-bearing features (e.g., fracture zones) that were not conduits. Sawyer et al. (2015) injected a salt solution into a sinkhole that drained to the conduit, then corroborated the conduit location by time-lapse ER combined with real-time monitoring of electrical conductivity in a monitoring well.

METHODS

In present study we used the electrical resistivity (ER) and self-potential (SP) methods in an attempt to locate the karst conduit within the Royal Spring groundwater basin.

Electrical resistivity data acquisition and processing

In this method, artificially generated current is injected into the ground through a pair of metal electrodes (current electrodes) and the resulting potential difference is measured by another pair of electrodes (potential electrodes). Various electrode configurations have been proposed by many researchers. The Wenner and Schlumberger arrays have been the most popular. In Wenner array, the electrodes are spread at uniform distance along a line with the current electrodes at the two ends and the potential electrodes in the middle of the array. All four electrodes are extended away from a fixed center with equal electrode spacing for depth exploration (sounding) while all four electrodes are moved along a line with constant electrode separation for mapping. In the Schlumberger array, the distance between the potential electrodes placed at the middle of the array is much less than the distance between the current electrodes at both ends. The Wenner array is commonly

used to map the lateral variation while the Schlumberger array is mostly used to explore greater depths.

We collected resistivity data at three different sites within the Inner Bluegrass region (Fig. 1). Resistivity data along two lines at each site were collected using an eight-channel SuperSting (R8/IP) multi-electrode earth resistivity meter, a product of Advanced Geosciences Inc. (AGI, Austin, Texas, USA). The two lines at the first site (Fig. 1) were surveyed at 2m electrode spacing and the other four resistivity lines at the remaining two sites were surveyed at 3m electrode spacing. The survey lines were expected to run perpendicular to the inferred trunk conduit. The relative distances between the current and potential electrode pairs were increased for each measurement in order to sample greater depth. The maximum separation between current and potential dipole was set at six times the dipole (current or potential) spacing for data with better resolution (Loke 2001).

The electrical resistivity survey data obtained were processed using EarthImager 2D version 2.2.0 to obtain inverted resistivity sections for all the survey lines. EarthImager 2D is a professional (commercial) software for resistivity and IP inversion developed by AGI. The resistivity data file format collected by the SuperSting is directly compatible with this software. In the initial setting menu in the settings window, the definition of the y-axis and orientation of the vertical axis need to be set before reading the data file while other settings can be set after reading the data file. As a first attempt at noisy data removal the bad electrodes were identified and removed using the electrode editor submenu of the edit main menu. Thresholds for all the criteria of noisy data removal in the initial setting window were set. Any data beyond these thresholds will automatically be removed in the inversion. Noisy data can also be removed manually by selecting with mouse clicks and deleting the data. Damped least-squares, smooth model inversion and robust least-squares inversion are three available options in the software to invert the resistivity data. The robust inversion method was chosen for the inversion of the entire data set but the other two methods of inversion were also tested during data processing. The robust least-squares inversion method is more efficient in inverting noisy data as compared to the smoothness constrained least-squares inversion (Dahlin and Zhou 2004). In robust inversion the model is produced by minimizing the absolute value of data misfit (L1-norm), while in the smooth inversion it is obtained by minimizing the square of data misfit (L2-norm) (Dahlin and Zhou 2004).

The inversion process progresses iteratively by taking the average apparent resistivity pseudosection as a starting model, finding a best fit between measured and predicted resistivity values and finally producing the inverted resistivity section. In each iteration the model is adjusted to match the measured pseudosection utilizing a least-squares optimization technique (Roth and Nyquist 2003).

Self-potential data acquisition and processing

The SP method is very simple, cost-effective and less

sophisticated than other geophysical methods. This method measures the natural electrical potential of the ground surface generated by various sources. Clearly defined sources of the SP are mainly the fluid and heat fluxes, diffusion between regions of different chemical composition, and redox reactions between ore bodies and their surroundings (Fagerlund and Heinson 2003). Flow of fluids through the subsurface media produces electrokinetic or streaming potential that is different from areas without this kind of fluid movement. Similarly, diffusion and mineralization potentials are produced in areas with different chemical composition and mineralized ore bodies, respectively. The high sensitivity of SP method compared to other geophysical techniques, particularly in the measurement of streaming potential due to groundwater flow, has been found to be more efficient than any other geophysical techniques (Lange and Kilty 1991, Fagerlund and Heinson 2003, Stevanovic and Dragisic 1998, Aubert and Atangana 1996). We used the SP method because of its inferred sensitivity to groundwater flow within a conduit (For further details see Tripathi 2009).

SP measurement in the field is very simple compared to other geophysical methods. The gradient and the fixed-base survey configurations are the main configurations commonly used to collect SP data along a survey profile (Telford et al. 1983; Parasnis 1986; Corwin 1990). In the gradient array, the two non-polarizing electrodes are connected through a digital multi-meter with a fixed length cable and moved along the survey line. After each measurement, the trailing electrode occupies the position of leading electrode for the new measurements and the process is continued to cover the entire survey length. As its name suggests, the fixed-base survey is performed by keeping one electrode (reference or base electrode) at a fixed base station while the other electrode (roving electrode) is moved at a constant distance to cover the entire survey line. The fixed-base array has many advantages over the gradient array: it lowers the level of cumulative error, can be conducted by a single operator, offers flexibility in reoccupying the previous stations, and offers better data reproducibility because stations with anomalous readings can be repeated (Corwin 1990). We used the fixed-base configuration for all of our survey lines, moving the roving electrode every 3.05 m (10 feet) or 4.57 m (15 feet) from the previous station. The base electrode (reference electrode) is buried about 30 cm and the roving electrode was placed about 15 to 20 cm below the ground surface. The holes were watered only in case of extremely dry soil, taking caution not to generate any kind of infiltration effect, to make a good contact between the electrodes and the ground. Two lines at Site 1 were measured every 3.05 m and the other lines were measured every 4.57 m from the base station. The base station was reoccupied every half an hour to correct for possible electrode drift caused by the temporal effect. As reported by Ernstson and Scherer (1986), we also observed a direct temperature effect on the electrodes during the day, particularly during sunny days. We tried to avoid this effect by putting the electrodes in shade. The fluctuation in meter readings increased as we moved farther away from

the base station. At each station the minimum and maximum SP values were recorded for 2 to 3 minutes according to the site condition. The mean value is the representative SP for that station. The measurements were taken two to four times on different dates at each site.

The SP data were smoothed by taking the moving average of the SP value along each survey line. This technique filters the high frequency noise from the data. SP variations can be significant even for an hour-long survey (Corwin 1990). Therefore, we used the following equation to correct for temporal drift, which assumes a linear drift between successive base station readings (Wanfang et al. 1999):

$$V_{cj} = V_j - [V_{pi} + (T_j - T_{pi})(V_{ni} - V_{pi}) / (T_{ni} - T_{pi}) + V_o]$$

Where V_{cj} is drift-corrected SP; V_j is measured voltage at time T_j on line j ; V_{pi} and V_{ni} are previous and subsequent readings at base station i at times T_{pi} and T_{ni} , respectively; and V_o is the first base-station reading.

Where topography is irregular, the SP data vary inversely relative to changes in elevation (Telford et al. 1983; Ernstson and Scherer 1986; Aubert and Atangana 1996). We used the topographic correction method described by Wanfang et al. (1999) to remove the probable topographic effect on the data from site 3 at the Kentucky Horse Park, where topographic relief is 5.13 and 3.7 m for lines 5 and 6 respectively. Topographic effects for the other two sites were not calculated because relief at those sites is less than 1 m. The topographic effect for each SP data point is calculated using the equation below (Wanfang et al. 1999):

$$V_{jte} = K_j (h_j - h_{oj})$$

Where V_j is the potential at elevation h_j along line j ; K_j is the topographic correction factor; and h_{oj} is elevation of the first measurement.

The data obtained after processing were plotted against the distance along the survey line to get the final SP profile for analysis and interpretation.

INTERPRETATION AND DISCUSSION

Electrical resistivity data interpretation

The resistivity data were interpreted to reflect the subsurface based on the response of underlying material to the injected currents. In the past, the resistivity data plotted against the electrode spacing along the survey line were matched with theoretically calculated master curves to find the layer parameters such as apparent resistivity, layer thickness and the depth to the layer interface. Nowadays, with the development of sophisticated data acquisition and data processing techniques, it has become less time consuming and labor intensive to model the subsurface with resistivity data. As the measured apparent resistivity is the result of the cumulative effect of subsurface media, the inhomogeneous and anisotropic nature of real earth material introduces ambiguity in interpretation.

All the sounding data gathered from the field applying

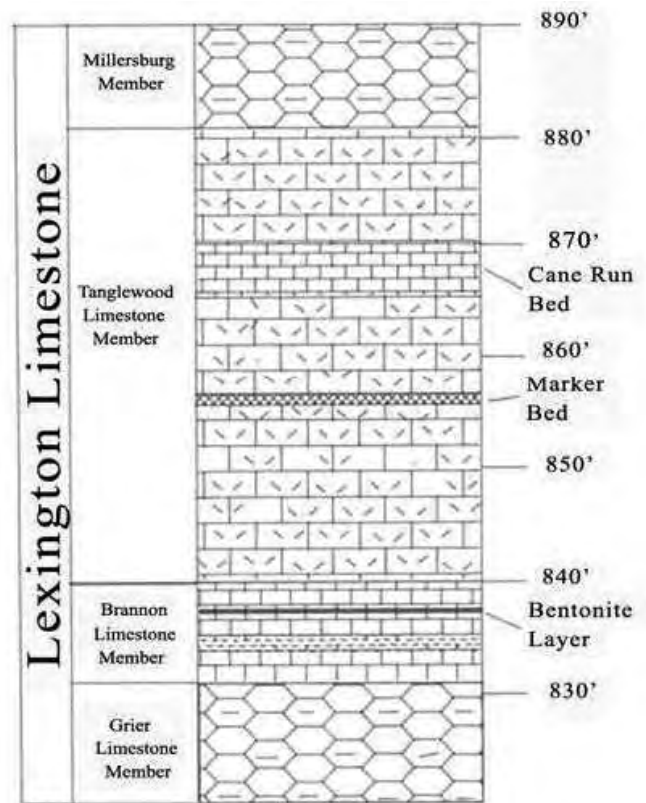


Fig. 2: Stratigraphic section measured in Vulcan quarry (Bonita 1993).

dipole-dipole electrode configuration were used to produce an inverted resistivity section along each survey profile. The inverted resistivity sections were interpreted on the basis of resistivity ranges that can be attributed to different earth materials. The average apparent resistivity values measured during this study and in the previous study (Graham 2000) are constraints to distinguish the anomaly from the background resistivity values. The area is predominantly underlain by the Lexington Limestone and the discontinuity in the high resistivity layer along the profile is interpreted as due to the change in rock mass qualities (such as fractures, moisture content etc.) along the profile. The average depth of penetration varies with the properties of overburden soil and, bedrock quality. The elevation changes between Royal Spring and the study sites are the major constraints to the probable target depths, i.e. the inferred conduit in the area.

Self-potential data interpretation

SP data were collected along ER lines at all three sites for comparison with ER responses. SP data were collected on multiple dates as a check on reproducibility. SP measurements were repeated at half-hour intervals at the base stations and used to correct for the electrode drift during the course of measurements. Moving averages for SP data were calculated to remove the high-frequency noise. The averaged data were plotted against the electrode spacing along each survey profile and the subsurface geology was interpreted based on negative or positive SP anomalies.

Comparison of ER and SP Results

UK Agricultural Research Farm (Site 1)

The inverted resistivity section and residual SP plot along line 1 (Fig. 3) at this site show a pronounced low resistivity and negative SP anomaly at approximately 14 m depth, between stations 60 to 70 m along the transect (Fig. 3). However, a hole drilled into this anomaly at 63.5 m did not encounter a solution conduit. The well log indicates that it could be a soil-filled sink-hole (James Dinger, Kentucky Geological Survey, personal correspondence). The identification of metallic objects in a hole dug during an SP survey is consistent with the negative SP response. Between stations 0 and 20 m, the data suggest very thin soil cover over weathered bedrock, which was subsequently verified by direct soil probes.

The sequence of 0–2 m thick low-resistivity overburden, a 2–3 m thick medium-resistivity layer and an 8–12 m thick high-resistivity layer closely correlates with the measured stratigraphic section in the nearby Vulcan Quarry (Fig. 2). The intermediate-resistivity layer can be correlated with the Millersburg Member and the high-resistivity layer can be correlated with the Tanglewood Member of the Lexington Limestone. The measured thicknesses for the Millersburg and Tanglewood members were 3.3 m and 12.1 m, respectively.

The inverted resistivity section and the SP plots show a pronounced anomaly at approximately 17 m depth between stations 40 and 50 m along line 2 (Fig. 4). However, a borehole drilled into the anomaly did not encounter a solution conduit.

The intermediate-resistivity layer (80 to 318 ohm-m) of 1 to 4 m thickness, below the low-resistivity overburden in the ER section, corresponds with the Millersburg Member in the measured section at the Vulcan Quarry (Bonita 1993). Similarly, the high-resistivity layer (318 to 530 ohm-m) of 5 to 10 m thickness below the intermediate-resistivity layer corresponds with the Tanglewood Member at the Vulcan Quarry (Bonita 1993).

Berea Road (Site 2)

The plots along line 3 (Fig. 5) at this site show a pronounced low resistivity and negative SP anomaly at approximately 16.6 m depth between stations 69 and 81 m (Fig. 5). Two holes (#1 at 72 m and #2 at 80 m along line 3) drilled into this target encountered a water-bearing conduit, whereas two holes drilled off the transect were dry. The static water levels measured (James Currens, Kentucky Geological Survey, personal communication) in both wells were 15.7 m below the ground surface. The target depth obtained from the ER section is about 5% higher than the measured depth in the well.

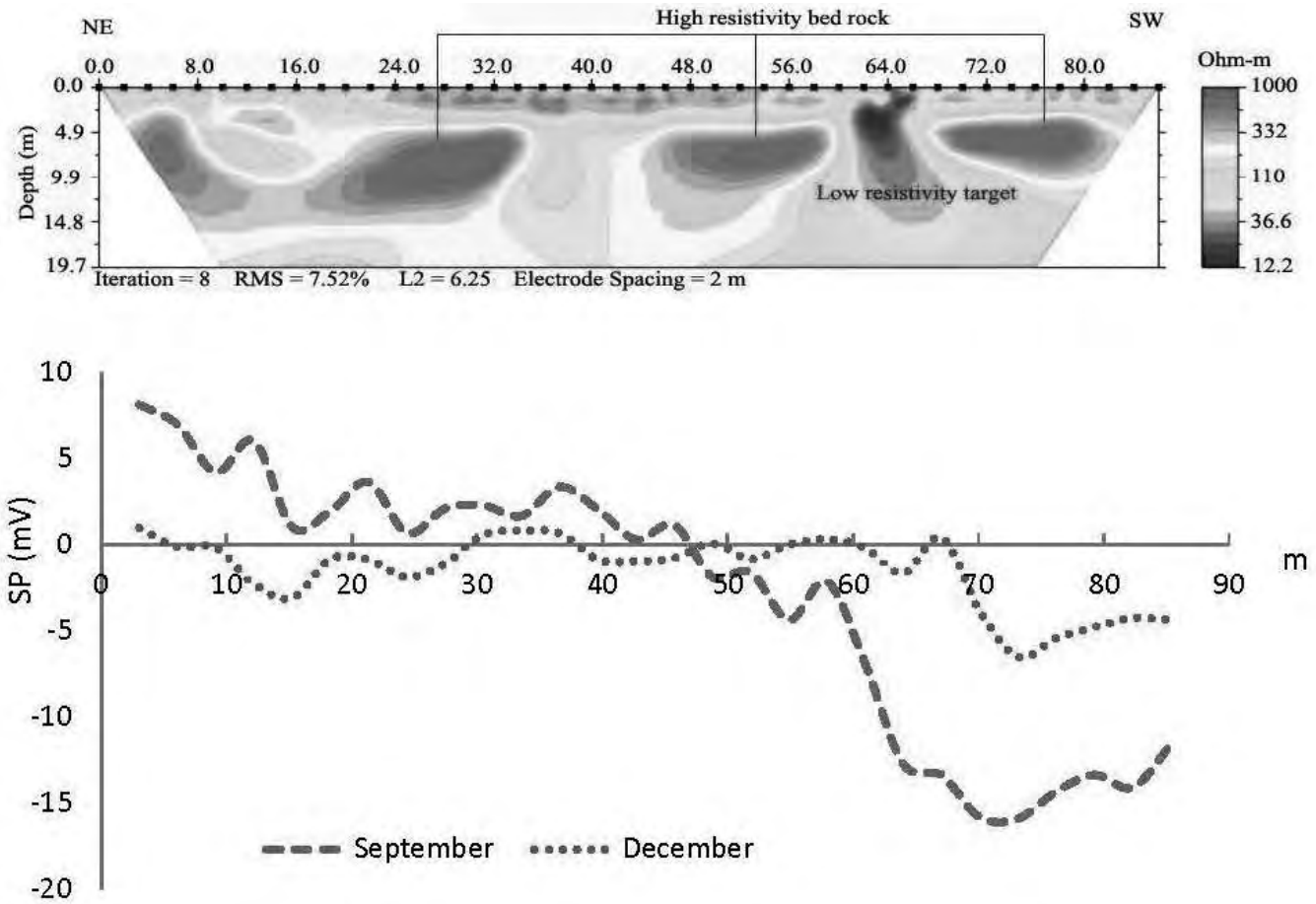


Fig. 3: ER and SP profiles along line 1 at the University of Kentucky Agricultural Research Farm (Site 1).

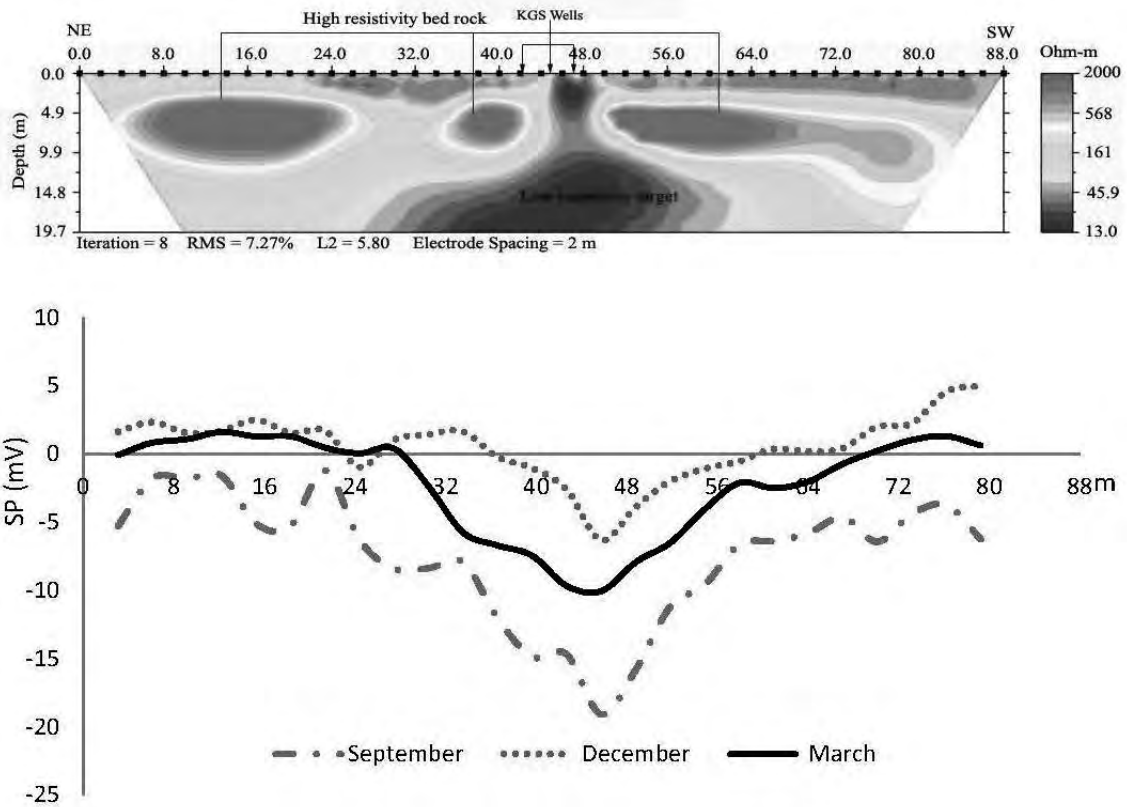


Fig. 4: ER and SP responses along line 2 at UK Agricultural Research Farm (Site 1).

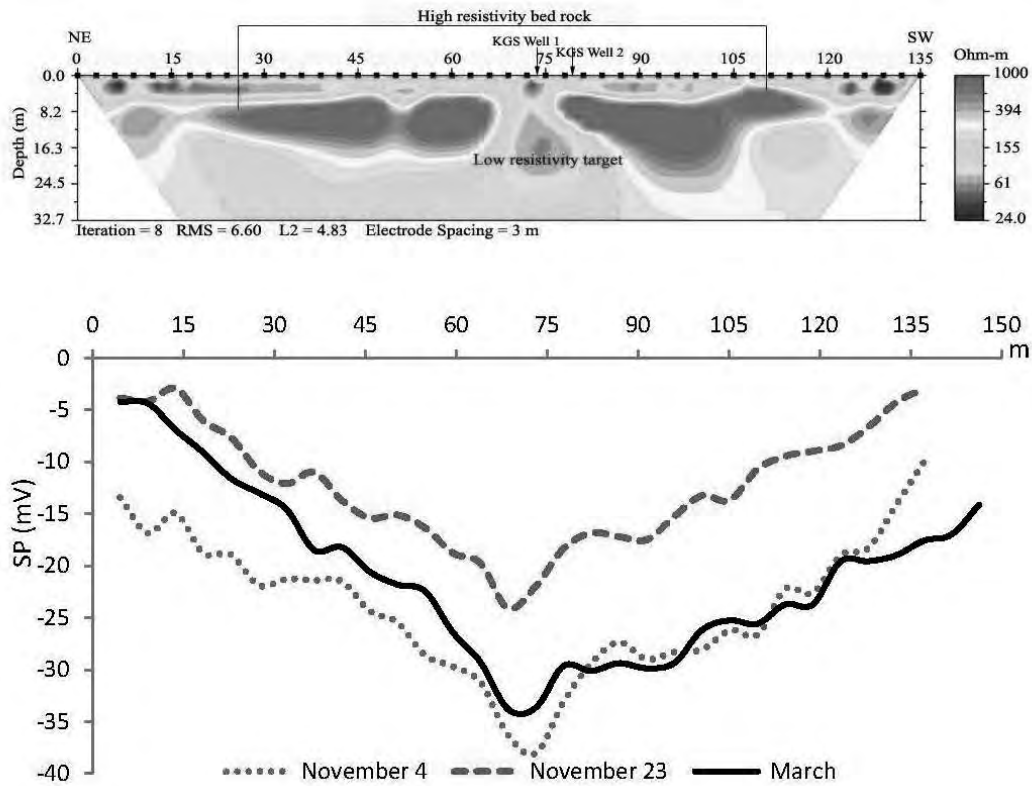


Fig. 5: ER and SP responses along line 3 at Berea Road (Site 2).

The ER section has been divided into low, medium and high-resistivity layers to a total depth of about 20 m. The low-resistivity layer at the top of the section is interpreted as soil overburden and might be the flood plain deposit of Cane Run. The second and third layers (with thicknesses of 3 and 12 m, respectively) may be correlated with the Millersburg and Tanglewood members of measured stratigraphic section at the Vulcan Quarry (Bonita 1993).

Kentucky Horse Park (Site 3)

The three low-resistivity anomalies along line 5 (Fig. 6) correspond roughly with the negative SP anomalies along the same line, although a fourth anomaly (at about 64 m along the transect) does not have a matching ER anomaly. The low-resistivity anomalies are located approximately at 17 m depth. The apparent resistivity for the anomaly located between stations 33 and 42 m is about 441 ohm-m, which exceeds the typical range for fresh groundwater; however, the high contrast between the anomaly and the background resistivity (1000 to 2000 ohm-m) could have a masking effect on the anomaly. The apparent resistivity is the volumetric average for the particular location and the surrounding high resistivity might have raised a true low resistivity value in this case. The second anomaly (345 ohm-m) is located between stations 75 and 108 m. The proximity of the low-resistivity anomaly at 123 m to a sinkhole and the typical sink-hole like ER response (Ahmed and Carpenter 2003, Jardani et al. 2007) suggest an ongoing process of sinkhole formation below ground surface. The top of the medium resistivity layer (200 to 520 ohm-m) in this section

is not distinct but the bottom of this intermediate layer is clear and continuous throughout the section. The thickness for the high resistivity (third) layer ranges from 5 to 15 m, which is equivalent to the thickness of the Tanglewood Member measured in the Vulcan Quarry (Bonita 1993). Along line 6, low ER signatures correspond with negative SP anomalies in most cases. However, the resistivity low (107.6 ohm-m) visible between stations 14 and 17 m along line 6(a) (Fig. 7) is not visible in the SP plots. The SP plots show an overall negative anomaly along approximately the middle third of the transect (Fig. 7). The resistivity low (around 500 ohm-m) located at about 15 m depth between stations 72 and 111 m (line 6(a)) was also reflected in the SP profile. The three wells (W-1, W-2 and W-3) drilled into this anomaly encountered water while a well (W-4) drilled slightly away, at station 68.58 m along the transect, was dry. Another ER anomaly at the SW end of line 6(a) was also drilled but the conduit was not encountered at the expected depth. This anomaly is located adjacent to a sinkhole and the resistivity signature could be the effect of ongoing sinkhole formation.

ER line 6(b) overlaps line 6(a) at station 84 m and continues toward the SW. The ER section shows distinct low-resistivity anomalies (around 200 ohm-m) between stations 99 to 126 m, located at a depth of 15 to 20 m, and below the station at 138 m, which might be a result of the nearby sinkhole. Similarly, the ER signature between stations 198 and 210 m at the SW end of the transect could also be a result of a sinkhole about 3 m away. The SP profiles also show negative anomalies for these targets, but they have not been drilled to verify the result.

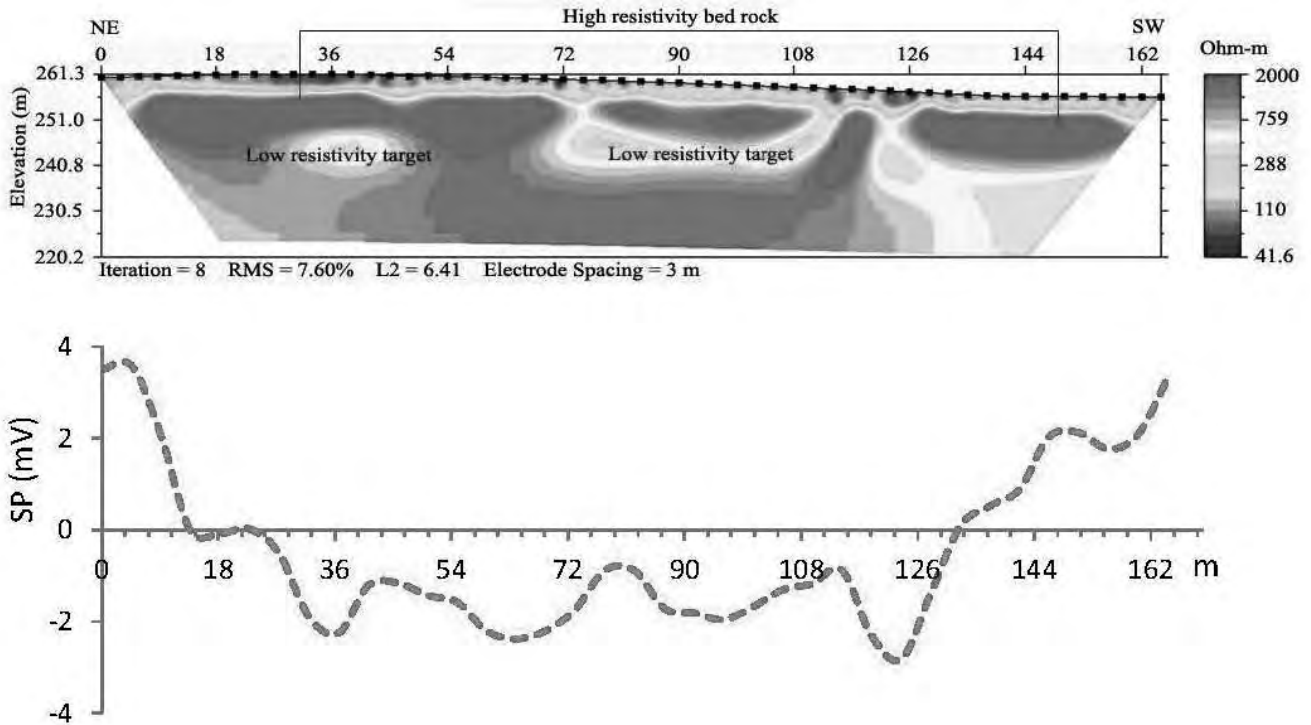


Fig. 6: ER and SP responses along line 5 at the Kentucky Horse Park (Site 3).

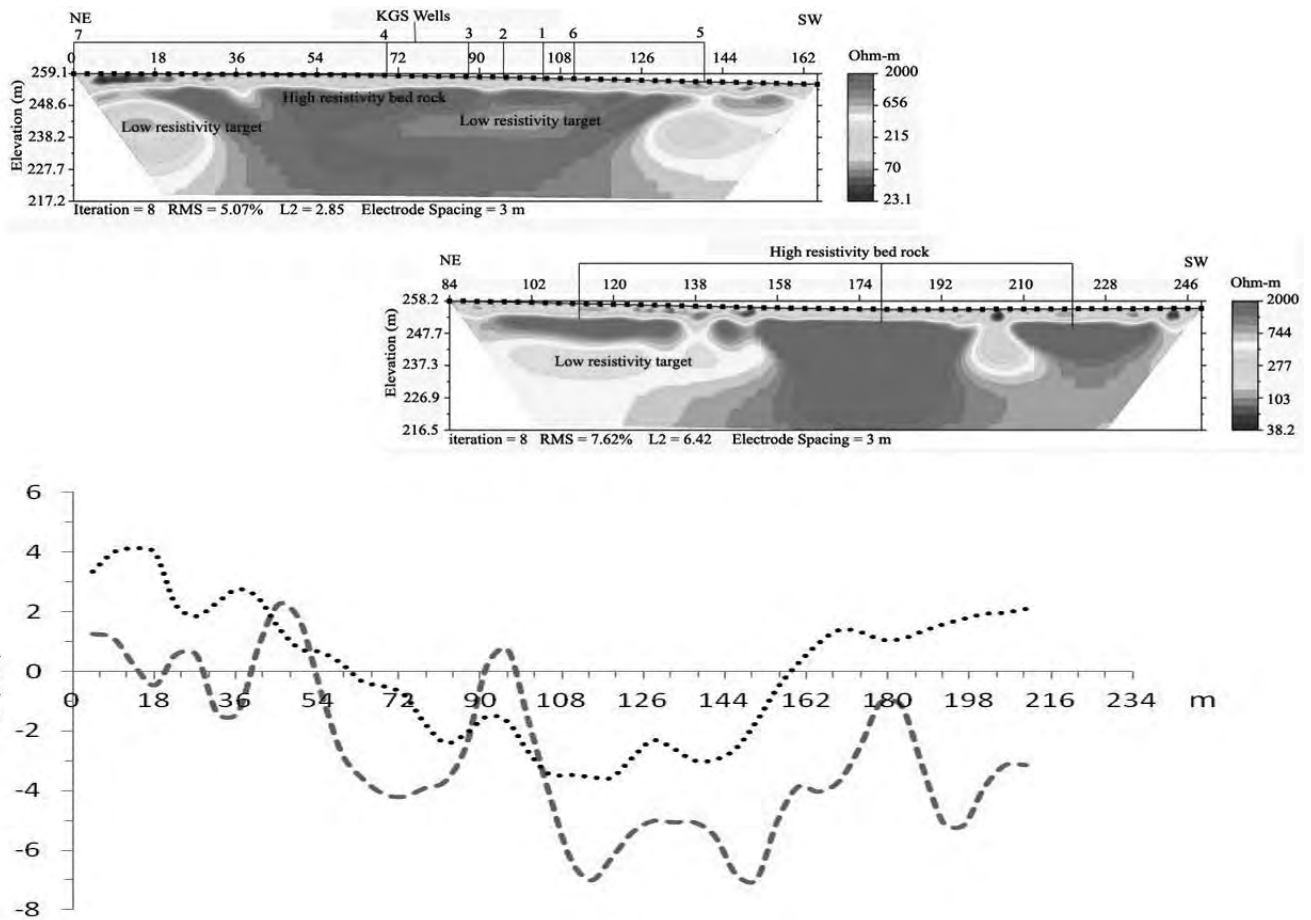


Fig. 7: ER and SP responses along line 6 at the Kentucky Horse Park (Site 3).

The upper 5 meters of the sections along lines 5 and 6 show similar ER responses of low to medium resistivity with discrete low-resistivity patches near the surface. The contact between the medium-resistivity layer and the underlying high-resistivity is located at a nearly uniform depth throughout the section, which suggests that the bedrock and the surface slope are dipping in the same direction. The high-resistivity layer for lines 6(a) and 6(b), with its top at about 5 m from the surface, can be correlated with the Tanglewood Member as at the other sites. The maximum soil (overburden) thickness at this site is perhaps 2 m from the surface. Consequently, the probable thickness for the medium-resistivity layer (about 3 m) is consistent with the Millersburg Member of the measured section (Bonita 1993).

Temporal variability in SP results

Qualitative comparison of profiles collected on different dates indicates that the relative magnitude of SP anomalies tends to vary with soil dryness. Excepting line 5, for which results were erratic, and line 3 on March 5, 2009, which was offset by 3 m from previous surveys, SP anomalies became less negative as one-week antecedent precipitation increased. Similarly, anomalies became less negative as temperature decreased (except for line 7, where the anomalies became more negative as both precipitation and temperature decreased

between August 29 and September 12, 2008). For lines 1, 2, 4, 6, and (considering the final two surveys) 7, the elapsed time between SP surveys spanned at least one season through the cool portion of the year (i.e., from late summer to early winter, early winter to late winter, autumn to late winter, or late summer to late winter). Consequently, the differences in SP responses may reflect not merely short-term (i.e., weekly) variability in weather, but also seasonal variability in soil moisture (i.e., soil moisture recharge during autumn, winter, and spring, Domenico and Schwartz 1998).

CONCLUSIONS

Six coincident ER and SP lines (86 to 249 m) and an additional SP line (230 m) were surveyed on different dates at three sites within the Inner Bluegrass karst region, Kentucky. The two different geophysical techniques were applied along coincident survey lines to correlate the interpreted results. The ER and SP methods complement each other in the delineation of anomalies that may correspond to karst conduits. Combined use of these methods can potentially decrease the ambiguities inherent in the geophysical data interpretation. In most of the cases, the low-resistivity anomalies are reflected as negative SP anomalies. Holes drilled into these anomalies along line 3 (between stations 69 and 81m along the transect) at Berea Road and along line 6 (between stations 72 and 111 m along

the transect) at the Horse Park sites encountered water-bearing conduits. The holes drilled over matched low-resistivity and negative SP anomalies at the University of Kentucky Agricultural Research Farm did not encounter the water-bearing target. However, the core log suggests the anomalies may represent sediment-filled sinkholes. SP data changed over time but the overall trends remained similar. In general, SP responses became less negative as precipitation increases and soil temperature decreases. Therefore, under wet field conditions, a negative SP anomaly generated by groundwater flow could be masked by the positive SP response generated by infiltration.

ACKNOWLEDGEMENTS

We would like to thank the UK College of Agriculture SB-271 program and Kentucky Geological Survey for their support to carry out this research. We are grateful to Dr. Edward Woolery for his guidance during ER data processing and Dr. James Dinger for coordinating the field work. We are equally thankful to Mr. John Warden, Dr. Estifanos Haile and Dr. Prakash Dhakal for their help at the different stages of this project. We are thankful to Dr. Pitambar Gautam and an anonymous reviewer for their meticulous review and comments.

REFERENCES

- Adeyemi, A., Idornigie, A. and Olorunfemi, M. 2006, Spontaneous potential and electrical resistivity response modelling for a thick conductor. *Jour. Appl. Sci. Res.*, v. 2, pp. 691-702.
- Advanced Geosciences, I. 2005, Instruction manual for the SuperStingTM with SwiftTM automatic resistivity and IP system: Austin, TX, Advanced Geosciences, Inc., 87 p.
- Ahmad, M. 1964, A laboratory study of streaming potentials. *Geophy. Prospec.*, v. 12, pp. 49-64.
- Ahmed, S. and Carpenter, P. 2003, Geophysical response of filled sinkholes, soil pipes and associated bedrock fractures in thinly mantled karst, east-central Illinois. *Environ. Geol.*, v. 44, pp. 705-716.
- Aubert, M. and Atangana, Q. 1996, Self-potential method in hydrogeological exploration of volcanic areas. *Ground Water*, v. 34, pp. 1010-1016.
- Bakalowicz, M. 2005, Karst groundwater: a challenge for new resources. *Hydrogeol. Jour.*, v. 13, 148-160.
- Bogoslovsky, V. and Ogilvy, A. 1972, The study of streaming potentials on fissured media models. *Geophy. Prospec.*, v. 20, pp. 109-117.
- Bonita, J.A. 1993, An electrical resistivity and fracture trace study in the Inner Bluegrass karst region of north-central Kentucky. University of Kentucky, M.S. Thesis, 155 p.
- Corwin, R. 1990, The self-potential method for environmental and engineering applications. *Geotech. Environ. Geophy.*, v. 1, pp. 127-145.
- Cressman, E. 1965, Geologic map of the Keene quadrangle, central Kentucky: U.S. Geological Survey Geologic Quadrangle Map GQ-440.
- Cressman, E. 1967, Geologic map of the Georgetown quadrangle, Scott and Fayette Counties, Kentucky: U. S. Geological Survey Geologic Quadrangle Map GQ-605.
- Dahlin, T. and Zhou, B. 2004, A numerical comparison of 2D resistivity imaging with ten electrode arrays. *Geophy. Prospec.*, v. 52, pp. 379-398.
- Domenico, P. A. and Schwartz, F. W. 1998, *Physical and Chemical Hydrogeology*: New York, John Wiley, 506 p.
- El-Araby, H. 2004, A new method for complete quantitative interpretation of self-potential anomalies. *Jour. Appl. Geophy.*, v. 55, pp. 211-224.
- Ernstson, K. and Scherer, H. 1986, Self-potential variations with time and their relation to hydrogeologic and meteorological parameters. *Geophy.*, v. 51, pp. 1967-1977.
- Fagerlund, F. and Heinson, G. 2003, Detecting subsurface groundwater flow in fractured rock using self-potential (SP) methods. *Environ. Geol.*, v. 43, pp. 782-794.
- Graham, C. D. R. 2000, Electrical resistivity studies in the Inner Bluegrass karst region, Kentucky. University of Kentucky, M.S. Thesis, 92 p.
- Hamilton, D. 1950, Areas and principles of ground-water occurrence in the Inner Bluegrass Region, Kentucky: Kentucky Geological Survey, Series 9. *Bull.*, 5, pp. 68.
- Ishido, T. and Mizutani, H. 1981, Experimental and theoretical basis of electrokinetic phenomena in rock-water systems and its applications to geophysics. *Jour. Geophy. Res.*, v. 86, pp. 1763-1775.
- Jardani, A., Dupont, J. and Revil, A. 2006, Self-potential signals associated with preferential groundwater flow pathways in sinkholes. *Jour. Geophy. Res.-Solid Earth*, v. 111, B09204.
- Jardani, A., Revil, A., Santos, F., Fauchard, C. and Dupont, J. 2007, Detection of preferential infiltration pathways in sinkholes using joint inversion of self-potential and EM-34 conductivity data. *Geophy. Prospec.*, v. 55, pp. 749-760.
- John, J. Q., David, T. and James, A. K. 2006, Modeling of complex flow in a karst aquifer. *Sed. Geol.*, v. 184, pp. 343-351.
- Kiraly, L. 2003, Karstification and groundwater flow. *Speleogenesis and Evolution of Karst Aquifers* 1.
- Lange, A. and Kilty, K. 1991, Natural-potential responses of karst systems at the ground surface. In *Proceedings of the Third Conference on Hydrogeology, Ecology, Monitoring, and Management of Hydrogeology in Karst Terrains*, pp. 179-196.
- Loke, M. 2001, Tutorial: 2-D and 3-D electrical imaging surveys. Geotomo Software, Malaysia.
- Matson, G. 1909, Water resources in the Blue Grass region, Kentucky: US Geological Survey Water Supply Paper, v. 233, pp. 42-45.
- Meyerhoff, S. B., Karaoulis, M., Fiebig, F., Maxwell, R. M., Revil, A., Martin, J. B. and Graham, W. D. 2012, Visualization of conduit-matrix conductivity differences in a karst aquifer using time-lapse electrical resistivity. *Geophy. Res. Let.*, v. 39, L24401.
- Motyka, J. 1998, A conceptual model of hydraulic networks in carbonate rocks, illustrated by examples from Poland. *Hydrogeol. Jour.*, v. 6, pp. 469-482.
- Nosow, E. and McFarlan, A. 1960, Geology of the central Bluegrass area. Kentucky Geological Survey, Univ. of Kentucky.
- Parasnis, D. 1986, *Principles of Applied Geophysics*, Chapman and Hall, New York, 402 p.
- Paylor, R. and Currens, J. 2004, Royal spring karst groundwater travel time investigation. Report prepared for Georgetown Municipal Water and Sewer Services, Kentucky Geological Survey, University of Kentucky, 15 p.
- Romanov, D., Dreybrodt, W. and Gabrovsek, F. 2002, Interaction of fracture and conduit flow in the evolution of karst aquifers. In Martin, J. B., Wicks, C. M., and Sasowsky, I. D. (eds.), *Hydrogeology and Biology of Post-Paleozoic Carbonate Aquifers*, Karst Waters Institute Special Publication 7, Charles Town, West Virginia.

- Roth, M. and Nyquist, J. 2003, Evaluation of multi-electrode earth resistivity testing in karst. *Geotech. Testing Jour.*, v. 26, pp. 167-178.
- Sawyer, A. H., Zhu, J., Currens, J. C., Atcher, C. and Binley, A. 2015, Time-lapse electrical resistivity imaging of solute transport in a karst conduit. *Hydrolog. Processes*, v. 29, pp. 4968-4976.
- Schwartz, B. and Schreiber, M. 2009, Quantifying potential recharge in mantled sinkholes using ERT. *Ground Water*, v. 47, pp. 370 - 381.
- Spangler, L., Troester, J. and Thraillkill, J. 1982, Groundwater in the Inner Bluegrass karst region, Kentucky. Research Report Available from the National Technical Information Service, Springfield VA 22161 as PB 83-108126.
- Stevanovic, Z. and Dragicic, V. 1998, An example of identifying karst groundwater flow. *Environ. Geol.*, v. 35, pp. 241-244.
- Sullivan, S. 1983, An investigation of flow in two groundwater basins in the Inner Bluegrass karst region, Kentucky using fluorescent dyes. University of Kentucky, M. S. Thesis, 85 p.
- Telford, W. M., Geldart, L. P., Sheriff, R. E. and Keys, D. A. 1983, *Appl. Geophy.* Cambridge University Press, New York, 760 p.
- Thraillkill, J. and Gouzie, D. 1984, Discharge and travel time determinations in the Royal Spring groundwater basin, Kentucky. Research Report Available from the National Technical Information Service, Springfield VA 22161 as PB 85-214765/AS.
- Thraillkill, J., Spangler, L., Hopper, W. and Troester, J. 1982, Groundwater in the Inner Bluegrass karst region, Kentucky. Research Report Available from the National Technical Information Service, Springfield VA 22161 as PB 83-108126.
- Thraillkill, J., Sullivan, S. B. and Gouzie, D. R. 1991, Flow parameters in a shallow conduit-flow carbonate aquifer, Inner Bluegrass karst region, Kentucky, USA. *Jour. Hydrology*, v. 129, pp. 87-108.
- Tripathi, G.N. 2009, Use of surface geophysical techniques to locate a karst conduit in the Cane Run – Royal Spring basin, Kentucky. University of Kentucky, M.S. Thesis, 115 p.
- UK Agricultural Weather Center, 2009, Climatology data. <http://www.agwx.ca.uky.edu/climdata.html>
- Wanfang, Z., Beck, B. and Stephenson, J. 1999, Investigation of groundwater flow in karst areas using component separation of natural potential measurements. *Environ. Geol.*, v. 37, pp. 19-25.
- White, W. 2002, Karst hydrology: recent developments and open questions. *Eng. Geol.*, v. 65, pp. 85-105.
- White, W. and White, E. 2005, Ground water flux distribution between matrix, fractures, and conduits: constraints on modeling. *Speleogenesis and Evolution of Karst Aquifers*, v. 3, pp. 2-8.
- Zhou, W., Beck, B. and Adams, A. 2002, Effective electrode array in mapping karst hazards in electrical resistivity tomography. *Environ. Geol.*, v. 42, pp. 922-928.
- Zhu, J., Currens, J. C. and Dinger, J. S. 2011, Challenges of using electrical resistivity methods to locate karst conduits – A field case in the Inner Bluegrass Region, Kentucky. *Jour. Appl. Geophy.*, v. 75, pp. 523-530.